



Indomethacin Treatment Post-irradiation Improves Mouse Parotid Salivary Gland Function via Modulation of Prostaglandin E₂ Signaling

Kristy E. Gilman^{1*}, Jean M. Camden², Lucas T. Woods², Gary A. Weisman² and Kirsten H. Limesand^{1*}

OPEN ACCESS

Edited by:

Fei Liu,
Texas A&M University, United States

Reviewed by:

Changyu Zheng,
National Institutes of Health,
United States
Sarah Knox,
University of California,
San Francisco, United States

*Correspondence:

Kristy E. Gilman
gilmankr@arizona.edu
Kirsten H. Limesand
limesank@u.arizona.edu

Specialty section:

This article was submitted to
Tissue Engineering and Regenerative
Medicine,
a section of the journal
Frontiers in Bioengineering and
Biotechnology

Received: 20 April 2021

Accepted: 28 June 2021

Published: 21 July 2021

Citation:

Gilman KE, Camden JM,
Woods LT, Weisman GA and
Limesand KH (2021) Indomethacin
Treatment Post-irradiation Improves
Mouse Parotid Salivary Gland
Function via Modulation
of Prostaglandin E₂ Signaling.
Front. Bioeng. Biotechnol. 9:697671.
doi: 10.3389/fbioe.2021.697671

¹ Department of Nutritional Sciences, University of Arizona, Tucson, AZ, United States, ² Department of Biochemistry and Christopher S. Bond Life Sciences Center, University of Missouri, Columbia, MO, United States

Annually, >600,000 new cases of head and neck cancer (HNC) are diagnosed worldwide with primary treatment being surgery and radiotherapy. During ionizing radiation (IR) treatment of HNC, healthy salivary glands are collaterally damaged, leading to loss of function that severely diminishes the quality of life for patients due to increased health complications, including oral infections and sores, cavities, and malnutrition, among others. Therapies for salivary hypofunction are ineffective and largely palliative, indicating a need for further research to uncover effective approaches to prevent or restore loss of salivary gland function following radiotherapy. Previous work in our lab implicated prostaglandin E₂ (PGE₂) as an inflammatory mediator whose release from radiation-exposed cells promotes salivary gland damage and loss of function. Deletion of the P2X7 purinergic receptor for extracellular ATP reduces PGE₂ secretion in irradiated primary parotid gland cells, and salivary gland function is enhanced in irradiated P2X7R^{-/-} mice compared to wild-type mice. However, the role of PGE₂ signaling in irradiated salivary glands is unclear and understanding the mechanism of PGE₂ action is a goal of this study. Results show that treatment of irradiated mice with the non-steroidal anti-inflammatory drug (NSAID) indomethacin, which reduces PGE₂ production via inhibition of cyclooxygenase-1 (COX-1), improves salivary gland function compared to irradiated vehicle-treated mice. To define the signaling pathway whereby PGE₂ induces salivary gland dysfunction, primary parotid gland cells treated with PGE₂ have increased c-Jun N-terminal Kinase (JNK) activation and cell proliferation and reduced amylase levels and store-operated calcium entry (SOCE). The *in vivo* effects of blocking PGE₂ production were also examined and irradiated mice receiving indomethacin injections have reduced JNK activity at 8 days post-irradiation and reduced proliferation and increased amylase levels at day 30, as compared to irradiated mice without indomethacin. Combined, these data suggest a mechanism whereby irradiation-induced PGE₂ signaling to JNK blocks critical steps in saliva secretion

manifested by a decrease in the quality (diminished amylase) and quantity (loss of calcium channel activity) of saliva, that can be restored with indomethacin. These findings encourage further attempts evaluating indomethacin as a viable therapeutic option to prevent damage to salivary glands caused by irradiation of HNC in humans.

Keywords: radiation, head and neck cancer, salivary glands, xerostomia, prostaglandin E₂, indomethacin, immunomodulation, regeneration

INTRODUCTION

Each year, >600,000 new cases of head and neck cancer (HNC) are diagnosed across the world (Johnson et al., 2020). Effective approaches to treat HNC include surgical excision of the tumor followed by IR, with or without chemotherapy (Cramer et al., 2019). During radiation treatment, salivary glands, located proximal to tumors, are collaterally damaged leading to reduced salivary gland function. Reduced saliva output causes numerous health complications, including increased rates of oral infections, cavities, and malnutrition and an overall poorer quality of life (Grundmann et al., 2009). Current treatment options for salivary hypofunction are palliative, relatively ineffective and costly to patients, indicating a need for further research to improve the quality of life for HNC patients (Jensen et al., 2019).

Wound healing is a complex regenerative process that occurs in three sequential but overlapping phases following tissue damage: (i) hemostasis/inflammation, (ii) proliferation/re-epithelialization, and (iii) remodeling. While each phase of the response is essential for adequate wound repair, dysregulation at any stage can lead to insufficient repair or chronic inflammation and excessive scarring. Hemostasis/inflammatory responses begin immediately following a wounding event and typically last for about 3 days (Reinke and Sorg, 2012). Radiation-induced inflammatory responses have been studied in salivary glands but present conflicting results (Jasmer et al., 2020). Research suggests that interleukin (IL)-6 mediates induction of cellular senescence in irradiated (13 Gy) submandibular glands (SMGs), with elevated levels seen at 3 h and 14 days post-IR. However, both IL-6 knockdown and IL-6 treatment prior to radiation exposure unexpectedly protected SMGs from senescence at 8 weeks post-IR, leaving the role of IL-6 during the inflammatory response to radiation difficult to understand (Marmary et al., 2016). Interestingly, treatment of SMGs with an adenovirus containing the neurotrophic factor, neurturin, prevents hypofunction in irradiated (6 Gy fractions × 5 days) salivary glands, when given pre- but not post-IR (Lombaert et al., 2020). Radiation treatment also resulted in a significant increase in inflammation-associated gene expression in irradiated mice (300 days post-IR) and minipigs (16 weeks post-IR) that was reduced by neurturin-expressing adenovirus administration prior to radiation exposure and was associated with normalized morphology and increased size and function of the salivary gland (Lombaert et al., 2020). In contrast, another study demonstrated that there is a decrease in immune-related gene expression and reduced macrophage numbers in irradiated (15 Gy) SMGs at days 7–28 post-IR, whereas adenoviral-induced

activation of the Sonic hedgehog (Shh) pathway at day 3 post-IR increased immune gene expression and macrophage numbers (Zhao et al., 2020). These studies suggest that an effective therapy to prevent salivary gland dysfunction due to radiation should target the hemostasis/inflammation phase of tissue damage, i.e., 0–3 days post-IR.

The second phase of the wound healing response, cell proliferation, is necessary to replace cells lost following damage; however, the homeostatic regulation of proliferation and differentiation is necessary to promote functional tissue repair. It has previously been proposed that the proliferative phase encompasses days 3–21 of the wound healing process, with transition to the remodeling phase occurring from day 21 through 1 year post-damage (Reinke and Sorg, 2012). In irradiated salivary glands, it has been shown that compensatory proliferation begins at day 5 post-IR and is mediated by activation of c-Jun N-terminal kinase (JNK) signaling (Wong et al., 2019). However, cell proliferation rates in irradiated salivary glands remain elevated compared to non-irradiated glands at chronic timepoints, days 30, 60, and 90 post-IR (Grundmann et al., 2010). Despite the increase in cell proliferation rates in irradiated salivary glands, the cells remain undifferentiated, as indicated by decreased amylase levels (Grundmann et al., 2010; Hill et al., 2014; Morgan-Bathke et al., 2014). Various pharmacological agents have been evaluated for restoration of irradiated parotid glands, where reducing the proliferative response correlates with increased salivary gland function *in vivo* (Grundmann et al., 2010; Hill et al., 2014; Morgan-Bathke et al., 2014). These data suggest that dysregulated signaling during the transition from the proliferative to remodeling phases of the wound healing process should be targeted to enhance salivary gland function following radiation damage.

The P2X7 receptor (P2X7R) for extracellular ATP released from damaged cells is a component of the innate immune system. Previous work from our lab showed that deletion or pharmacological antagonism of the P2X7R prevents salivary gland dysfunction in mice caused by radiation exposure (Gilman et al., 2019). Interestingly, mouse primary parotid gland cells lacking the P2X7R secrete significantly lower levels of the biologically active lipid, prostaglandin E₂ (PGE₂), basally and following radiation exposure, which suggests that P2X7R-mediated PGE₂ release may lead to salivary gland dysfunction that could be reversed by blocking the P2X7R (Gilman et al., 2019). PGE₂ is produced from plasma membrane phospholipid-derived arachidonic acid that is first converted to prostaglandin H₂ by cyclooxygenases (COXs), COX-1 and COX-2, and then to

PGE₂ by microsomal PGE synthase-1 (mPGES-1), mPGES-2 or cytosolic PGE synthase (cPGES) (Gilman and Limesand, 2020). PGE₂ acts by binding to four different E-prostanoid receptors (EPs), EP1-4R, to induce the activation of multiple G proteins (Gilman and Limesand, 2020). EPs, typically EP2R and EP4R, also can transactivate the epidermal growth factor receptor (EGFR) (Jiang et al., 2017). Based on their ability to activate G protein and EGFR signaling, PGE₂-bound EPs regulate multiple physiological processes, including, proliferation, differentiation, survival, cytokine production, immune cell migration and vasodilation/vasoconstriction (Dennis and Norris, 2015; Gilman and Limesand, 2020). PGE₂ also induces the phosphorylation of intracellular c-Jun terminal kinase (JNK) and its downstream target c-Jun (Zeng et al., 2015; Zhong et al., 2015), which we have previously shown mediates the induction of compensatory proliferation in irradiated salivary glands (Wong et al., 2019). Indomethacin is a non-steroidal anti-inflammatory drug (NSAID) that functions via nonselective and reversible inhibition of COXs to reduce the synthesis of eicosanoids, including PGE₂ (Lucas, 2016). Due to the postulated role of PGE₂ in the induction of radiation-induced salivary gland dysfunction, we evaluated the hypothesis that indomethacin treatment would restore irradiated salivary gland function by blocking PGE₂ production and subsequent activation of JNK-mediated compensatory proliferation.

MATERIALS AND METHODS

Mice

Animals were maintained according to the University of Arizona Institutional Animal Care and Use Committee (IACUC) regulations with protocols approved by the IACUC. Four to eight week-old C57BL/6J (stock no. 000664) or FVB/NJ mice (stock no. 001800) were purchased from Jackson Labs (Bar Harbor, ME, United States). Age- and sex-matched mice of the same genotype were randomly assigned to treatment groups. Mice were on 12 h light/dark cycles and housed in vented cages with food and water *ad libitum*. Where indicated, mice received intraperitoneal (IP) injections of vehicle (sterile saline with 10% ethanol) or indomethacin (1 mg/kg body weight, Sigma, no. I7378, St. Louis, MO, United States) prepared from a 10 mg/mL stock solution in 100% ethanol, warmed at 55°C for 5 min, diluted to 1 mg/mL in saline and sterilized by passage through a 0.22 μm Polyvinylidene difluoride (PVDF) filter.

Radiation Treatment

Mice were sedated via an IP injection of a mixture of ketamine/xylazine (50–10 mg/kg), constrained in 50 mL tubes and shielded with >6 mm lead, leaving only the head and neck region exposed. Mice or cells were placed in the radiation field and received a single 5 Gy dose of radiation from a ⁶⁰Co Teletherapy unit at 80 cm distance from the source and ~0.3–0.4 Gy/min (Theatron-80, Atomic Energy of Canada, Ottawa, ON, Canada) or a 225 kV X-ray unit at 48 cm distance from the source and 1.4 Gy/min (RS2000, Rad Source Technologies, Buford, GA, United States).

Saliva Collection

Salivary flow rates were evaluated on days 3, 10, or 30 following radiation. Saliva production was stimulated with an IP injection of carbachol (0.25 mg/kg body weight) and whole saliva was collected for 5 min via vacuum aspiration into pre-weighed tubes and then snap-frozen. Salivary flow was calculated by taking the difference in tube weight (post-collection minus pre-collection) and dividing by 5 min to express saliva secretion in milligrams per minute. Saliva flow rates were normalized to the average of the non-irradiated, vehicle-injected group on each day of collection.

Primary Cell Preparation

Parotid glands were removed from four to eight week-old C57BL/6J mice, prepared as previously described (Gilman et al., 2019) and suspended in primary cell culture media: DMEM/F12 containing (in wt/vol, except where noted) epidermal growth factor (0.4%; Fisher Scientific), insulin (0.125%; Invitrogen), glutamine (1.25%; Invitrogen), nonessential amino acids (1%; Invitrogen), transferrin (0.125%, Invitrogen), retinoic acid (0.05%; Sigma-Aldrich), trace elements (1%; Thermo Fisher Scientific), gentamycin (0.5%; Thermo Fisher Scientific), fungizone (0.2%; Invitrogen), hydrocortisone (0.04%; Sigma-Aldrich), and fetal bovine serum (10% vol/vol; Thermo Fisher Scientific, unless the use of serum-free media was indicated). Cells were used immediately as dispersed parotid cell aggregates or seeded onto 35 mm collagen-coated plates and grown for 2 days prior to use. Primary parotid cells or aggregates from independent preparations are considered as a single replicate for assays and at least three replicates were performed from separate preparations for all experiments.

Cyclooxygenase Activity Assay

Primary cells were prepared as described above. On day 2 of culture, cells were treated with indomethacin (25 μM in saline from the 100% ethanol stock solution) or vehicle (saline with 0.1% ethanol) and cells were collected 24 h later. Protein was extracted as described below and COX activity was measured via a COX activity assay (Abcam, no. ab204699, Cambridge, United Kingdom) following the manufacturer's instructions.

Prostaglandin E₂ Enzyme-Linked Immunosorbent Assay

Primary cells were prepared as described above. On day 2 of culture, media was replaced and cells were treated with indomethacin (25 μM in saline) or vehicle (saline with 0.1% ethanol) 1 h prior to receiving a 5 Gy dose of radiation. Cell-free supernatants were collected at indicated timepoints following radiation and the PGE₂ concentrations were determined with an enzyme-linked immunosorbent assay (PGE₂ ELISA, R&D Systems, no. KGE004B, Minneapolis, MN) following the manufacturer's instructions, where PGE₂ was normalized to the protein concentration of the corresponding cell culture dish.

Prostaglandin E₂ Treatment

Vehicle (DMSO) or varying doses (10 nM, 100 nM, 1 μM, 10 μM) of PGE₂ (Cayman Chemical, no. 14010, Ann Arbor, MI,

United States) were diluted in serum-free primary cell media and used to treat dispersed parotid cell aggregates at the indicated timepoints for dose-response and kinetic analyses. For amylase staining, PGE₂ was diluted to 10 μM in serum-complete primary cell media and cells were treated on culture plates for 24 h prior to collection. Cells were centrifuged and resuspended in lysis buffer to extract proteins as described below.

Protein Isolation and Quantification

Parotid glands were harvested and snap-frozen from untreated and irradiated mice at day 8 or 30 post-IR. Tissues were homogenized in radioimmunoprecipitation assay (RIPA) buffer, with protease inhibitor cocktail (30 μL/mL; Sigma, no. P8340), sodium orthovanadate (5 mM) and phenylmethylsulfonyl fluoride (PMSF, 1 mM). Tissue homogenates were incubated on ice for 30 min, sonicated for 1–2 min and centrifuged at 12,000 RPM for 10 min at 4°C to remove cell debris. Cells or aggregates were collected by scraping, centrifuged, resuspended in tissue protein extraction reagent (T-PER, Thermo no. 78510) with protease inhibitor cocktail (30 μL/mL), sodium orthovanadate (5 mM), and PMSF (1 mM), incubated on ice for 10–15 min and centrifuged at 12,000 rpm for 10 min at 4°C to remove cell debris. Protein content was measured with the Pierce Coomassie Plus Bradford assay (Thermo, no. 23236, Waltham, MA, United States) or the Bicinchoninic acid (BCA) assay (Thermo, no. 23225).

Immunoblotting

Five to fifty micrograms of protein were added to 2X Laemmli sample buffer and boiled for 5–10 min at 95–100°C. Sample proteins were separated via electrophoresis on 10% polyacrylamide gels. Proteins were transferred to PVDF membranes (Millipore, no. IPVH00010) at 100 volts for 1 h. Membranes were blocked in either 5% (w/v) nonfat milk or 5% (w/v) bovine serum albumin (BSA, Fisher Bioreagents, no. BP1600-100) dissolved in tris-buffered saline with Tween 20 (TBS-T, 20 mM Tris base, 137 mM NaCl, 0.05% Tween 20 (v/v), pH 7.6) for 1 h at room temperature, washed in TBS-T three times for 5 min each and incubated in primary antibody overnight at 4°C. The following rabbit-anti-mouse primary antibodies were used: phospho-JNK/SAPK (p54/p46)^{T183/Y185} (1:1,000, Cell Signaling, no. 4668, Danvers, MA, United States), JNK/SAPK (p54/p46, 1:1,000, Cell Signaling, no. 9252) phospho-c-Jun^{S73} (1:1,000, Abcam, no. ab30620), c-Jun (1:1,000, Cell Signaling, no. 9165), amylase (1:3,000 in 3% BSA, Sigma, no. A8273), Aquaporin 5 (AQP5; 1:1,000, Millipore-Sigma, no. AB3559-50UL), muscle, intestine and stomach expression 1 (MIST1; 1:1,000, Cell Signaling, no. 14896), EP1 (1:500; Cayman Chemical no. 101740), EP2 (1:200; Cayman Chemical no. 101750), EP3 (1:200; Cayman Chemical no. 101760), EP4 (1:200; Cayman Chemical no. 101775), ERK1/2 (1:1,000; Cell Signaling, no. 9102) or β-tubulin (1:1,000, Cell Signaling, no. 2128). Membranes were washed three times for 5 min each in TBS-T then incubated in HRP-conjugated goat anti-rabbit IgG antibody (1:10,000 in 5% nonfat milk TBS-T; Cell Signaling, no. 7074S) for 1 h at room temperature. Membranes were washed three times for 5 min each in TBS-T then incubated with Pierce ECL Western Blotting

Substrate (Thermo, no. 32109) for 1 min or SuperSignal West Pico Plus Chemiluminescent Substrate (Thermo, no. 34577) for 5 min. Membranes were exposed to autoradiography film (Genesee, no. 30-810) and developed using an Srx-101A X-ray film processor (Konica). Membranes were stripped using Restore Western Blotting Stripping Buffer (Fisher, no. 21063), blocked in 5% nonfat milk and re-probed for loading controls. Densitometry was performed using ImageJ software (NIH).

5-Ethynyl-2'-Deoxyuridine Incorporation Assay

Primary parotid gland cells were prepared as described above and were cultured on 18 mm collagen-coated glass coverslips (Neuvitro, no. H-18-collagen, Vancouver, WA, United States). On day 4 of culture, cells were treated with vehicle (DMSO), PGE₂ (Cayman Chemical, no. 14010), or EP receptor-selective (EP1R-EP4R) agonists at indicated doses: 17-phenyl trinor PGE₂ (EP1R agonist; Cayman Chemical, no. 14810), AH13205 (EP2R agonist; Santa Cruz Biotechnology, no. sc-214513), sulprostone (EP3R agonist; Cayman Chemical, no. 14765) and CAY10598 (EP4R agonist; Cayman Chemical, no. 13281). Cells were serum-starved for 2 h prior to treatment. All compounds were solubilized in DMSO, mixed into serum-free primary cell culture media (described above) and cells were treated for 24 h. During the last hour of EPR agonist treatment, cells were incubated with 5-ethynyl-2'-deoxyuridine (EdU) from the Click iT EdU cell proliferation kit (Invitrogen, no. 10337). EdU was fluorescently labeled following the manufacturer's instructions. Coverslips were mounted on glass slides with Prolong Gold Antifade Mountant (Thermo Fisher Scientific, no. 36934). Images were captured on a Leica DM5500 fluorescence microscope (Leica Microsystems, Wetzlar, Germany) with 4-megapixel Pursuit camera (Diagnostic Instruments, Inc.) at 200× magnification. EdU positive cells and total cells were manually counted. Groups were quantified by averaging the number of positive cells out of the total number of cells from 5 fields of view/slide and 3 slides per treatment. Graphs depict the average number of positive cells/total number of cells. Each symbol represents an independent sample.

Intracellular Calcium Quantification

Intracellular free Ca²⁺ concentration ([Ca²⁺]_i) in isolated parotid epithelial cells was quantified as previously described (Woods et al., 2018). Briefly, primary parotid gland cells untreated or treated with 10 μM PGE₂ for 24 h in serum-free DMEM/F12 media containing gentamycin (50 μg/ml) were washed with assay buffer (120 mM NaCl, 4 mM KCl, 1.2 mM KH₂PO₄, 1.2 mM MgSO₄, 1 mM CaCl₂, 10 mM glucose, 15 mM HEPES, 1% (w/v) BSA, pH 7.4) and then adhered to chambered coverslips using Cell-Tak cell adhesive (Corning Inc., Corning, NY, United States) and loaded with 2 μM of the calcium indicating dye, fura-2-AM (Life Technologies, Carlsbad, CA, United States) in assay buffer for 30 min at 37°C, washed and incubated in dye-free assay buffer for 30 min. Prior to use, cells were washed again and placed in calcium-free assay buffer containing 0.2 mM EDTA and baseline fluorescence values were

collected for 60 s prior to stimulation with carbachol (100 μ M) for 210 s to evaluate muscarinic type 3 receptor functionality. Then, 3 mM calcium was added for the final 90 s to quantitate store-operated calcium entry (SOCE) into cells. Changes in the 340/380 nm fluorescence excitation ratio (505 nm emission) were detected using an InCyt Dual-Wavelength Fluorescence Imaging System (Intracellular Imaging, Cincinnati, OH, United States). Resulting fluorescence ratios were converted to $[Ca^{2+}]_i$ (nM) using a standard curve created with solutions containing known concentrations of Ca^{2+} .

Histology

Salivary glands were harvested from mice at indicated timepoints post-IR and submerged in 10% neutral buffered formalin overnight. Tissues were sent to IDEXX Bioanalytics (Columbia, MO, United States) for processing where they were dehydrated with ethanol and xylene, embedded in paraffin and sectioned at 4 μ m.

Immunofluorescence

Salivary gland sections were incubated at 37°C for 20 min, submerged in Histoclear (National Diagnostics, no. HS-200) for 10 min and rehydrated in ethanol gradations (100, 95, 70, and 50%) and deionized water for 10 min each. Sections were permeabilized for 15 min in 0.2% (v/v) Triton X-100 in PBS, then washed with PBS three times for 5 min each. Next, antigen retrieval was completed by microwaving sections in citric acid (pH 6.0) for 10 min and then cooling for 20 min. Sections were washed with PBS three times for 5 min each, blocked in 0.5% New England nuclear blocking agent (Perkin Elmer, no. 2346249) for 1 h at room temperature and then incubated in anti-amylase antibody (1:1,000 in 1% BSA; Sigma, no. A8273) or anti-Ki67 antibody [1:400 in 1% BSA, Cell Signaling, no. 9129] overnight at 4°C. Slides were washed three times for 10 min each, incubated in fluorophore-conjugated goat anti-rabbit IgG antibody (Alexa Fluor 488, 1:500 in 1% BSA; Thermo, no. A-11008) for 1 h at room temperature, washed again three times for 10 min each and then rinsed in water for 5 min. Cell nuclei were stained with 4',6-diamidino-2-phenylindole (DAPI, 1 μ g/mL; Invitrogen, no. D1306) for 3 min then washed with water for 10 min. Amylase-stained sections were mounted with 50% glycerol in 10 mM Tris-HCl (pH 8.0), and Ki67-stained sections were mounted with ProLong Gold Antifade mounting agent (Invitrogen, no. P36934) and imaged the following day. Images were captured on a Leica DM5500 with 4-megapixel Pursuit camera at 400 \times magnification with identical camera settings used for all images. Quantification was done using ImageJ software with images from 20 fields of view per mouse with 5 mice per treatment for amylase area, or 5 fields of view per mouse with 4 mice per treatment for Ki67. Graphs depict the mean percentage of amylase positive area or the average percentage of Ki67 positive cells out of the total cell number. Each point represents an independent mouse.

Statistical Analysis

Statistical tests were run using GraphPad Prism 9 software (San Diego, CA, United States). Normally distributed data was assessed by Brown-Forsythe test. To determine significance

between groups, a student's *t*-test, or a one-way analysis of variance (ANOVA) was used, followed by Dunnett's *post hoc* comparisons when comparing to a control group, or Bonferroni's *post hoc* comparisons when comparing all groups. A *p*-value of less than 0.05 is considered statistically significant. Specific *p*-values are indicated by the number of asterisks above groups (**p* < 0.05, ***p* < 0.01, ****p* < 0.001, *****p* < 0.0001).

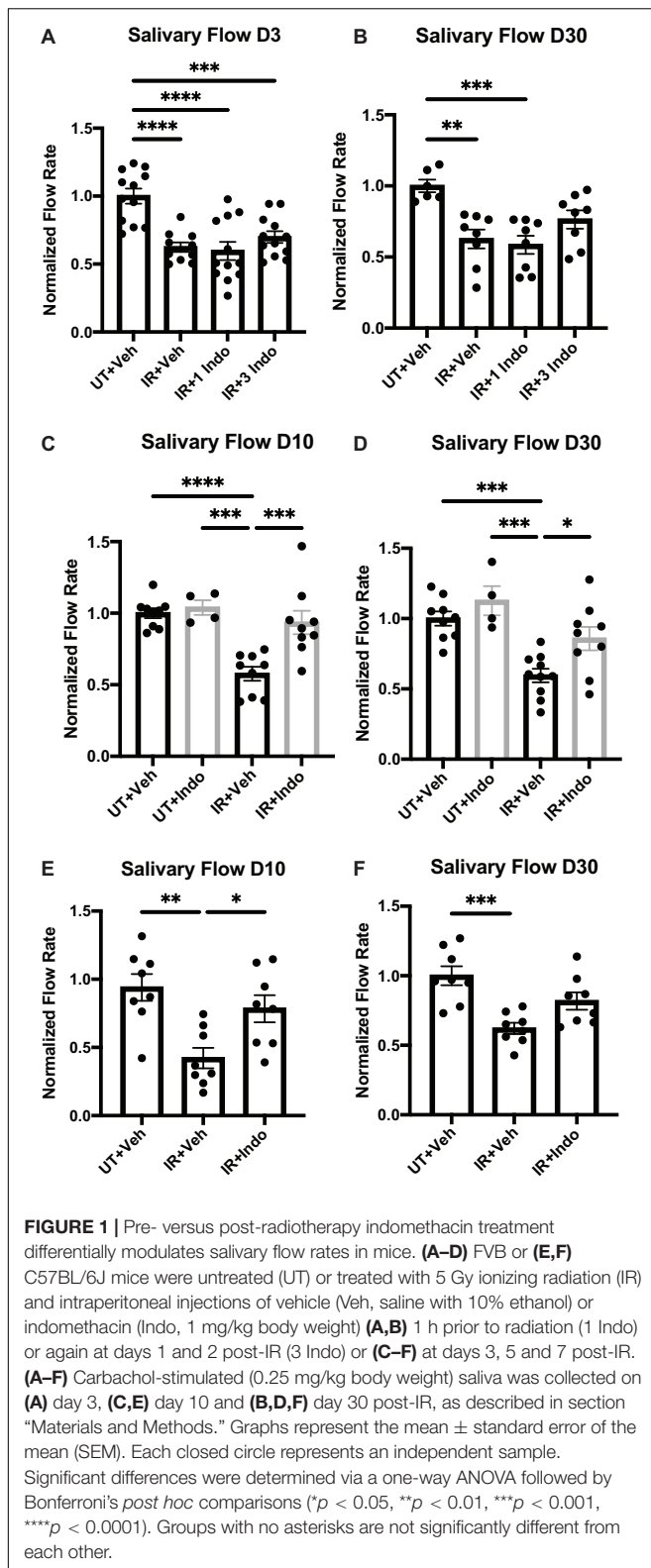
RESULTS

Post-radiation Indomethacin Treatment Restores Salivary Gland Function in Mice

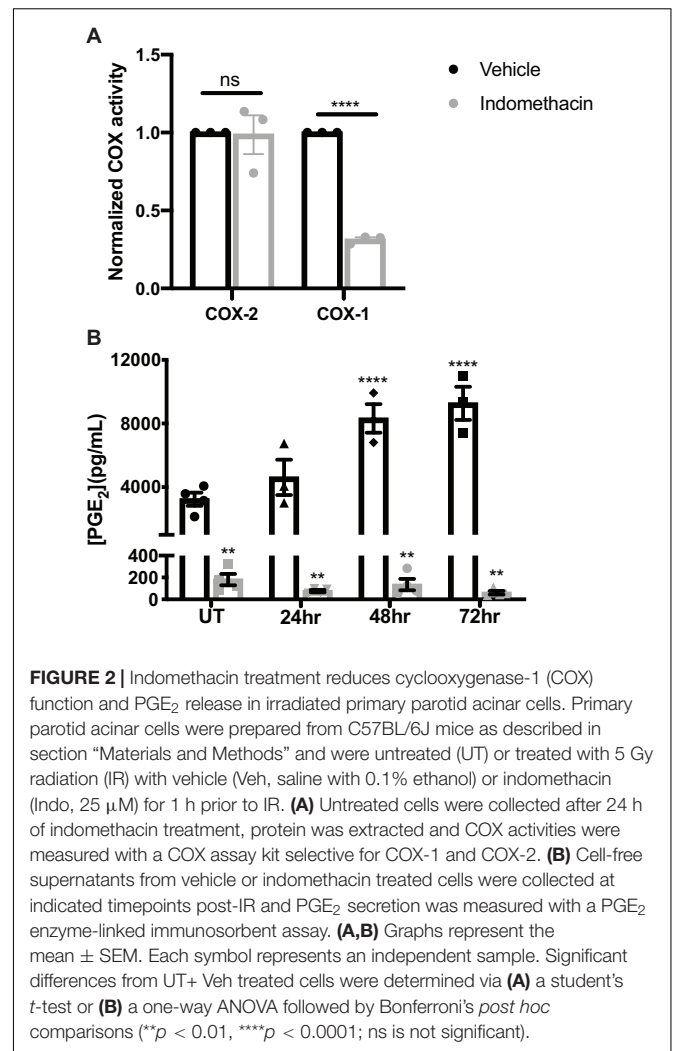
FVB/NJ (Figures 1A–D) or C57BL/6J (Figures 1E,F) mice were exposed to 5 Gy of radiation and were injected with the NSAID, indomethacin (1 mg/kg body weight), 1 h prior to IR only (Figures 1A,B, IR+1 Indo) or again at days 1 and 2 post-IR (Figures 1A,B, IR+3 Indo). Alternatively, mice received injections of indomethacin at days 3, 5, and 7 post-IR (Figures 1C–F). Stimulated salivary flow rates were measured on day 3, representative of an acute timepoint post-IR damage, and day 30, representative of a chronic timepoint post-IR damage (Grundmann et al., 2010). The results indicate that a single injection of indomethacin (1 Indo) prior to IR exposure does not preserve salivary gland function post-IR (Figures 1A,B). Interestingly, mice receiving both pre- and post-IR indomethacin (3 Indo) injections have reduced stimulated saliva output on day 3 that is only modestly improved by day 30 (Figures 1A,B). In contrast, FVB/NJ (Figures 1C,D) and C57BL/6 (Figures 1E,F) mice receiving indomethacin injections on days 3, 5, and 7 post-IR (Figures 1C–F) show salivary flow rates at days 10 and 30 post-IR similar to untreated, vehicle injected (UT+Veh) mice (Figures 1C,D). In addition, indomethacin treatment alone does not alter salivary gland function in mice not treated with IR (Figures 1C,D). Combined, these data suggest that inhibiting eicosanoid synthesis with indomethacin following radiation exposure leads to restoration of salivary gland function.

Indomethacin Treatment of Primary Parotid Gland Cells Reduces COX-1 Activity and Prostaglandin E₂ Secretion Induced by Radiation

Indomethacin inhibits both COX-1 and COX-2 functions (Tanaka et al., 2002), but has greater selectivity for COX-1 (Warner et al., 1999; Brown et al., 2001). To evaluate whether indomethacin is COX-1- or COX-2-selective in salivary glands, parotid acinar cells were treated with vehicle or indomethacin (25 μ M) for 24 h and COX-1 and COX-2 activities were measured. Results indicate that indomethacin preferentially inhibits COX-1 in primary parotid acinar cells (Figure 2A). We have previously shown that there are elevated levels of PGE₂ secreted from primary parotid gland cells following IR exposure, with lower PGE₂ levels detected in IR-exposed P2X7R^{-/-} cells that correlate with improved salivary gland function (Gilman et al., 2019). To determine if indomethacin treatment modulates PGE₂ secretion, primary parotid gland cells were exposed to



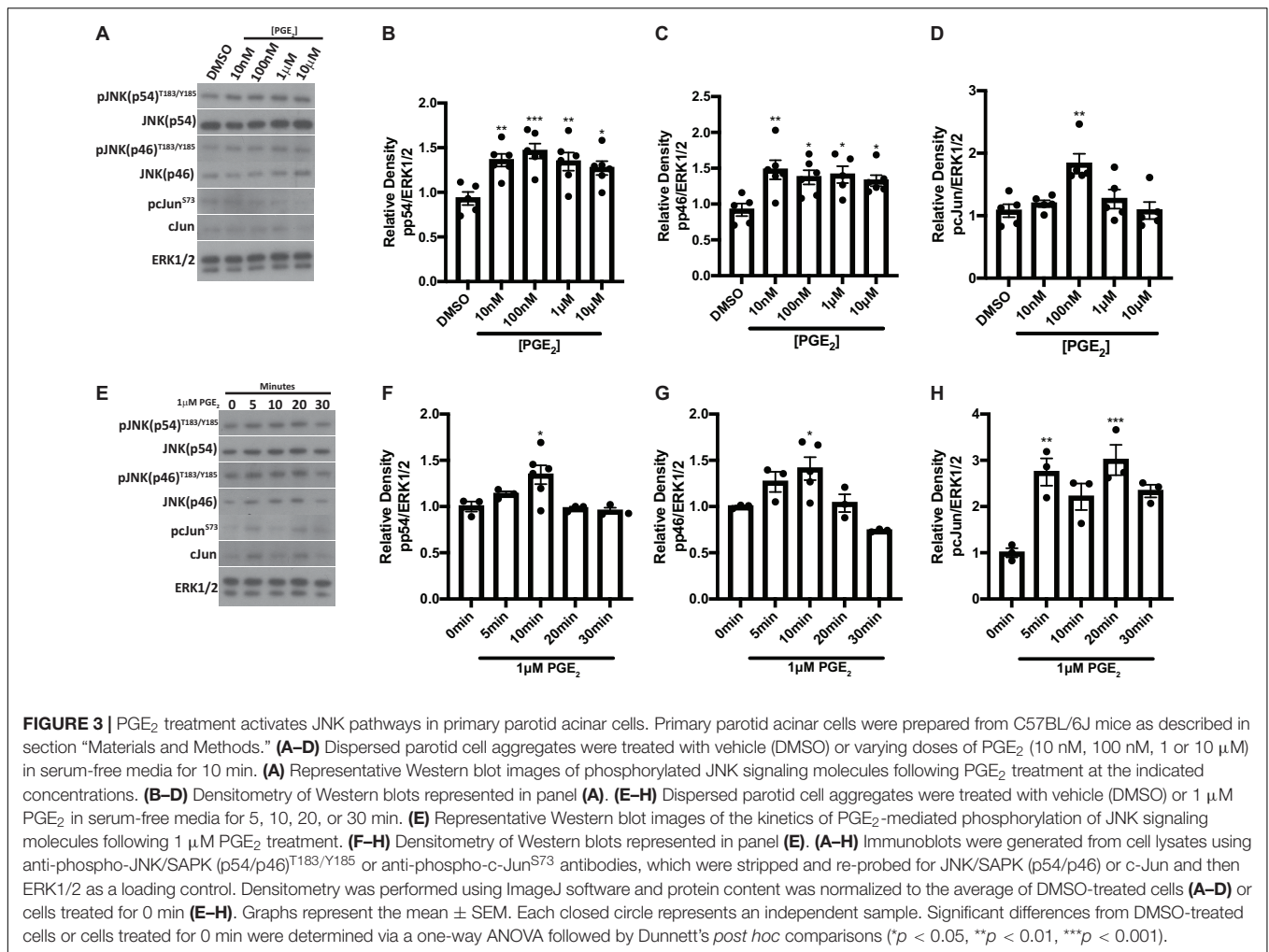
5 Gy radiation with or without indomethacin pre-treatment (25 μM). Results indicate that indomethacin significantly reduces PGE₂ secretion into primary parotid cell-free supernatants at



24–72 h post-IR, whereas PGE₂ secretion is also inhibited by indomethacin in cells not treated with IR (Figure 2B). These data show that indomethacin functions by inhibiting COX-1 activity and reduces constitutive and radiation-induced production of PGE₂ in primary parotid gland cells.

Prostaglandin E₂ Treatment Activates JNK Signaling in Primary Parotid Gland Cells

We have previously shown that the JNK pathway is activated at day 5 post-IR and promotes radiation-induced compensatory cell proliferation that correlates with the loss of saliva secretion (Grundmann et al., 2010; Hill et al., 2014; Wong et al., 2019). PGE₂ has been shown to stimulate JNK and c-Jun phosphorylation in human endometrial stromal cells (Zeng et al., 2015) and primary human skin fibroblasts (Arasa et al., 2019). To evaluate whether PGE₂ activates JNK signaling in salivary glands, primary parotid cell aggregates were treated with varying doses of PGE₂ for 10 min and phosphorylation of the JNK p54 and p46 isoforms and their downstream target, c-Jun, were assessed

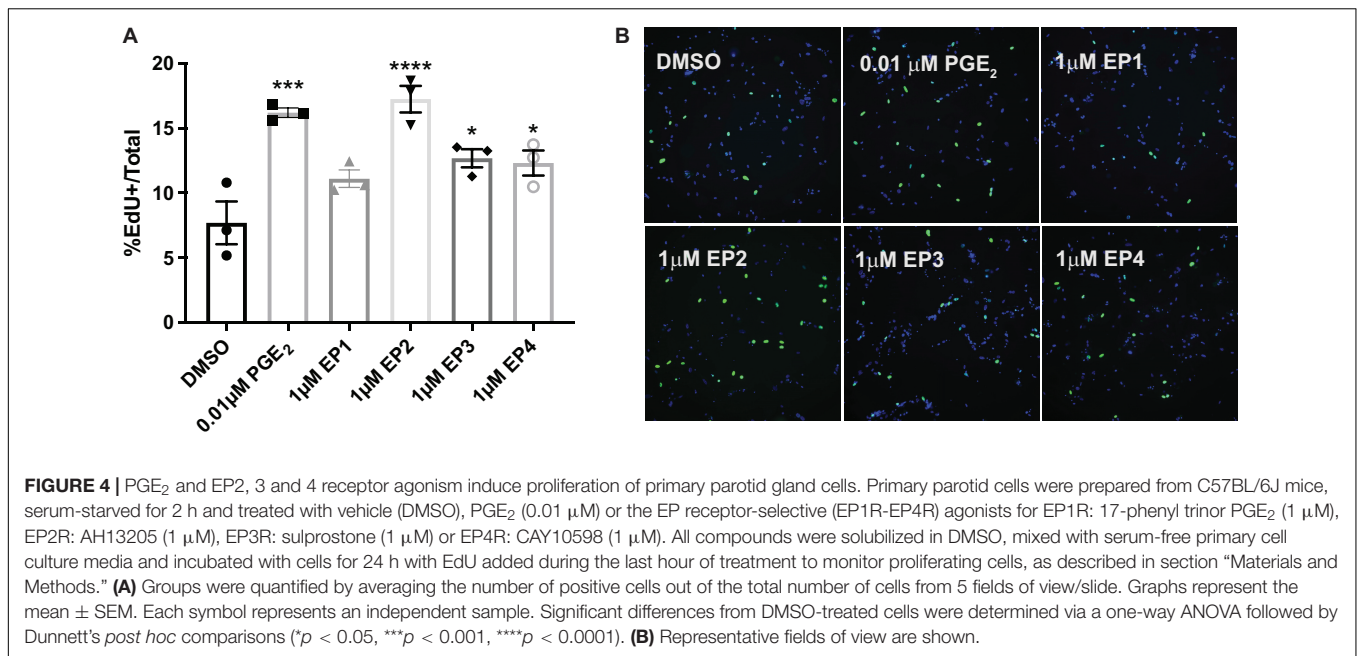


via Western analysis. Phosphorylation of both p54 and p46 JNK are enhanced following treatment with all doses of PGE₂ tested (Figures 3A–C), whereas c-Jun phosphorylation is modestly increased following 100 nM PGE₂ treatment (Figures 3A,D). To determine kinetic changes in JNK and c-Jun phosphorylation induced by PGE₂, primary parotid cell aggregates were treated with 1 μM PGE₂ and phosphorylation of JNK p54 and p46 and c-Jun were assessed after 0, 5, 10, 20, and 30 min. Results indicate that phosphorylation of p54 and p46 JNK are elevated at 10 min following 1 μM PGE₂ treatment (Figures 3E–G). Interestingly, c-Jun phosphorylation is increased at all timepoints measured, with significantly higher levels observed at 5 and 20 min following PGE₂ treatment as compared to the 0 timepoint (Figures 3E,H). These data show that PGE₂ activates the JNK/c-Jun pathway in parotid glands.

Prostaglandin E₂ and EP2, 3, and 4 Receptor Agonism Induce Proliferation of Primary Parotid Gland Cells

It has been shown that JNK activation mediates compensatory proliferation in parotid glands at day 5 post-IR

(Wong et al., 2019) and PGE₂-induced JNK signaling is able to stimulate proliferation of pulmonary epithelial tumor cells (Zhong et al., 2015) and human mesenchymal stem cells (Yun et al., 2011). To evaluate whether PGE₂ treatment or selective EP receptor (EP1R-EP4R) activation is able to induce cell proliferation in salivary glands, primary parotid gland cells were treated with PGE₂ or selective agonists for EP1R (17-phenyl trinor PGE₂; 1 μM), EP2R (AH13205; 1 or 10 μM), EP3R (sulprostone; 0.01 or 1 μM) or EP4R (CAY10598; 1 or 10 μM) for 24 h and EdU incorporation was determined during the last hour of treatment as a measure of cell proliferation. The number of EdU positive cells increases following PGE₂ treatment (0.01 or 0.03 μM), EP2R agonism (1 or 10 μM AH13205), EP3R agonism (0.01 or 1 μM sulprostone) or EP4R agonism (1 or 10 μM CAY10598) as compared to DMSO-treated cells (Figures 4A,B and Supplementary Figures 1A,B). EP1R agonism (1 μM 17-phenyl trinor PGE₂) did not increase proliferation levels compared to DMSO-treated controls (Figures 4A,B). These data indicate PGE₂ increases proliferation in parotid gland cells via either EP2, 3 or 4 receptor activation, which is likely mediating the induction of the compensatory proliferation response seen post-IR (Grundmann et al., 2010; Hill et al., 2014;



Wong et al., 2019), downstream of radiation-induced PGE₂ secretion (Gilman et al., 2019).

Prostaglandin E₂ Decreases Amylase Levels and Store-Operated Calcium Entry in Primary Parotid Cells

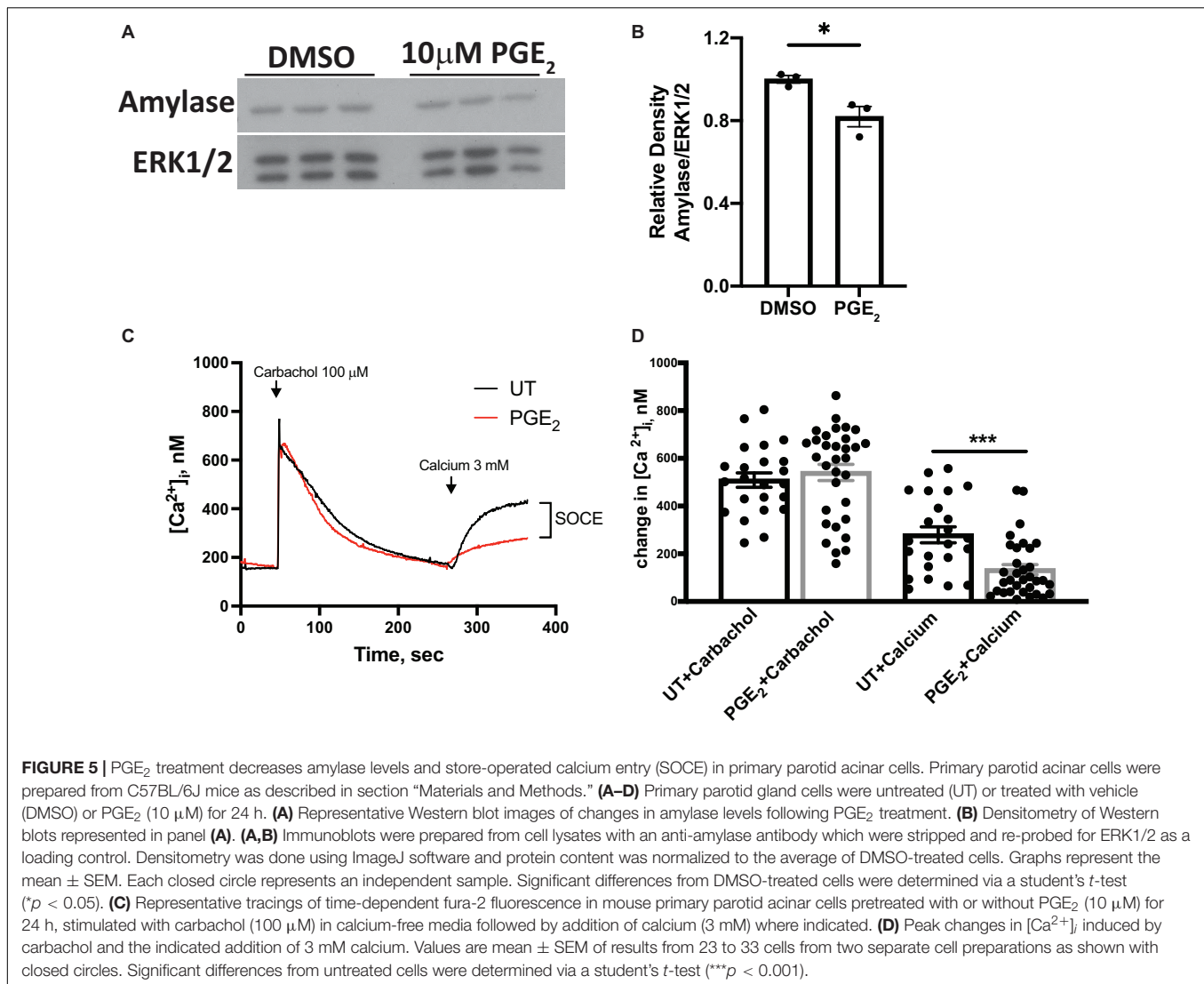
Amylase is a marker for differentiated acinar cells and, following radiation damage, amylase levels are reduced in parotid glands, which correlates with reduced gland function (Grundmann et al., 2010; Hill et al., 2014; Morgan-Bathke et al., 2014). To evaluate whether PGE₂ influences amylase production in parotid glands, primary parotid cells were treated with 10 μM PGE₂ for 24 h and amylase levels were determined via Western analysis. Amylase levels are reduced in PGE₂-treated cells when compared to vehicle-treated cells (Figures 5A,B). To identify other mechanisms by which PGE₂ mediates alterations in salivary gland function, primary parotid cells were treated with PGE₂ for 24 h and loaded with the calcium indicating dye, fura-2. Intracellular calcium concentration ($[Ca^{2+}]_i$) was measured for 6 min following carbachol (100 μM) stimulation in media lacking calcium, and 3 mM calcium was added 4.5 min after carbachol stimulation. The peak $[Ca^{2+}]_i$ in parotid gland cells following carbachol stimulation is not different between vehicle and PGE₂-treated cells, indicating normal functionality of muscarinic type 3 receptors on parotid cells and no effect of PGE₂ on the $[Ca^{2+}]_i$ in intracellular stores (Figures 5C,D). Following addition of 3 mM calcium into the media, there is reduced re-entry of calcium in PGE₂-treated cells indicated by a reduction in $[Ca^{2+}]_i$ as compared to vehicle-treated cells, suggesting that PGE₂ signaling blocks SOCE in parotid glands (Figures 5C,D). Taken together, these data illustrate that PGE₂ reduces amylase levels and inhibits SOCE in primary parotid cells.

Indomethacin Treatment Reduces JNK Signaling *in vivo* at Day 8 Post-IR

We have previously shown that IR activates JNK signaling 5 days post-IR, which partially regulates the compensatory proliferation response in parotid glands (Wong et al., 2019). It is well described that JNK activation induces c-Jun phosphorylation (Johnson and Nakamura, 2007). To determine if indomethacin treatment modulates JNK signaling *in vivo*, mice with or without 5 Gy IR exposure were injected with vehicle or indomethacin (1 mg/kg body weight) at days 3, 5 and 7 post-IR. Parotid glands were harvested at day 8 and used for immunoblots. Phosphorylation of JNK p54 and p46 are increased in irradiated parotid tissues at day 8 post-IR, a response reduced with indomethacin treatment (Figures 6A–C). Further, phosphorylation of c-Jun that is significantly increased at day 8 post-IR is reversed with indomethacin treatment (Figures 6A,D). These data illustrate that post-IR indomethacin treatment blocks JNK activation in parotid glands, supporting a role for indomethacin in protection from IR-induced salivary gland damage.

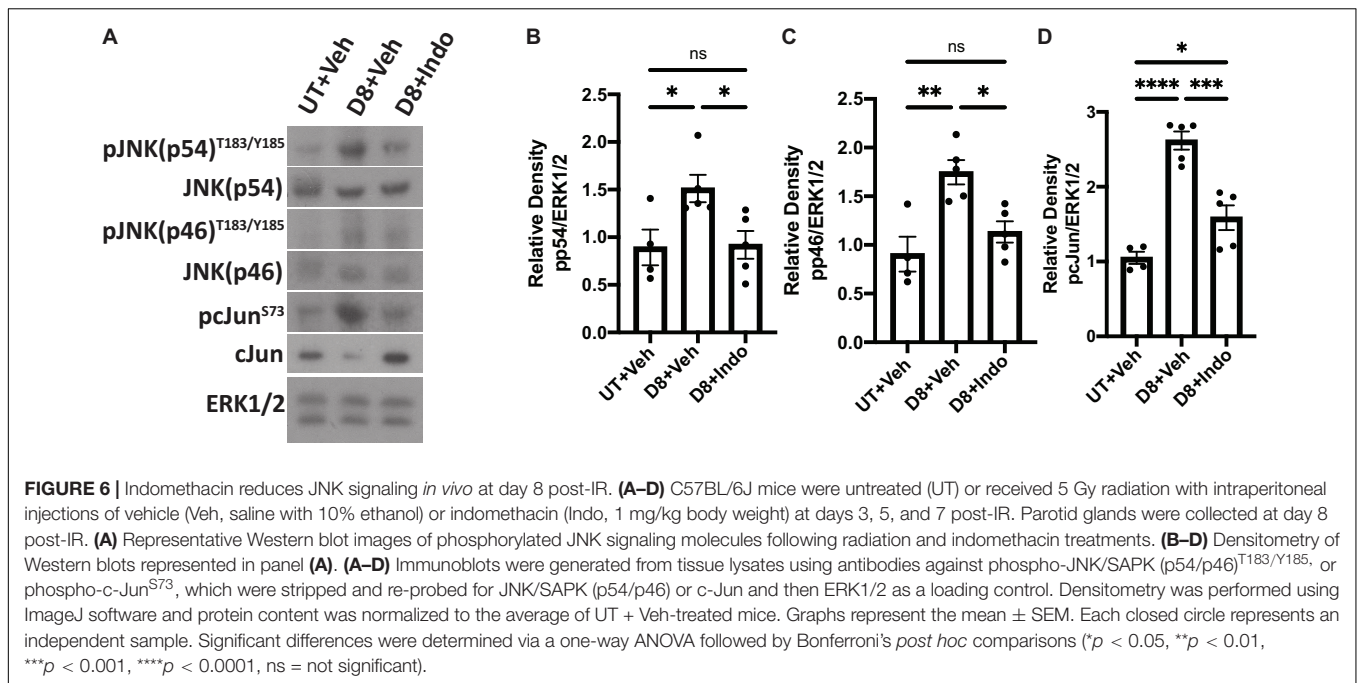
Post-radiation Indomethacin Treatment Enhances Parotid Gland Amylase Levels and Reduces Compensatory Proliferation at Day 30

To confirm the *in vitro* findings that PGE₂ decreases amylase secretion, mice were untreated or exposed to 5 Gy radiation with vehicle or indomethacin injections at days 3, 5, and 7 post-IR and parotid glands were collected at day 30, representing a chronic timepoint following damage (Grundmann et al., 2010). Protein was extracted for immunoblot analysis, which shows that total amylase levels are reduced in irradiated, vehicle-injected mice (Figures 7A,B), whereas indomethacin treatment



increases amylase levels in irradiated mice to similar levels as unirradiated, vehicle-injected mice (Figures 7A,B). To confirm these findings and evaluate the proportion of amylase producing acinar cells *in vivo*, parotid glands were collected at day 30 for histological analysis and immunohistochemistry was used to determine the area of salivary gland tissue staining positive for amylase (graphed as percent of total area). The proportion of amylase secreting acinar cells is reduced at day 30 in irradiated, vehicle-injected mice, but indomethacin restored amylase levels to those in unirradiated, vehicle-injected mice (Figures 7C,D). To evaluate whether or not indomethacin exerts modulatory effects on other proteins that influence salivary gland secretion, whole tissue homogenates were used for immunoblots to assess levels of aquaporin 5 (AQP5) and muscle, intestine, and stomach expression 1 (MIST1). Irradiated, vehicle-injected mice have reduced levels of AQP5 in parotid gland homogenates when compared to untreated glands, with indomethacin-treated glands having levels that were not statistically different from either group (Supplementary Figures 2A–C). Unexpectedly,

MIST1 levels were not significantly different across treatment groups (Supplementary Figures 2A–C). PGE₂ is able to induce proliferation following EP2-4 activation (Figure 4 and Supplementary Figure 1) and compensatory proliferation that occurs in irradiated salivary glands correlates with loss of function (Grundmann et al., 2010; Hill et al., 2014; Morgan-Bathke et al., 2014). However, the evaluation of indomethacin as a compensatory proliferation modulator post-radiation has not been previously explored. Parotid gland tissue sections were stained for the proliferation marker Ki67 to evaluate differences in compensatory proliferation following radiation in vehicle and indomethacin-treated mice. Ki67 positive cells are significantly increased in irradiated, vehicle-injected mice and reduced with post-radiation indomethacin treatment (Figures 7E,F). These data demonstrate that indomethacin treatment reduces the compensatory proliferation response and increases the concentration of the major enzyme amylase in irradiated parotid glands indicating improved differentiation of acinar cells, which suggests that this pharmaceutical should be further tested for



restoration of the normal protein composition of saliva in patients undergoing radiotherapy for HNC.

DISCUSSION

Wound healing is a highly complex process that requires delicately coordinated signaling for adequate repair to occur. In irradiated salivary glands, there is conflicting data regarding induction of inflammatory responses (Marmary et al., 2016; Lombaert et al., 2020; Zhao et al., 2020). However, it is well characterized that excessive cell proliferation occurs, but without adequate production of functional differentiated cells (Grundmann et al., 2010; Hill et al., 2014; Morgan-Bathke et al., 2014), suggesting that inhibition of the pathways responsible for compensatory proliferation may improve salivary gland function post-IR. Indomethacin is an NSAID that inhibits both COX-1 and COX-2 functions, but COX-1 has a 10-fold lower IC₅₀ value for indomethacin than COX-2 (COX-1 IC₅₀: 13 nM; COX-2 IC₅₀: 130 nM) (Warner et al., 1999). These findings are consistent with our data from primary parotid gland cells, where 25 μM indomethacin caused a significant reduction in COX-1 activity after 24 h but had no effect on COX-2 activity (Figure 2A). Our previous studies demonstrated reduced PGE₂ secretion from primary parotid gland cells of P2X7R^{-/-} compared to wild type mice that correlated with the preservation of salivary gland function post-IR, although the differences observed in expression levels or activity of COX isoforms did not correlate with changes in PGE₂ secretion (Gilman et al., 2019). Here, we show that indomethacin reduces PGE₂ production and secretion in both untreated and irradiated primary parotid cells, which correlates with reduced COX-1 activity (Figures 2A,B). PGE₂ has many physiological roles

under homeostatic and inflammatory conditions. However, in the context of radiation damage to salivary glands, the generation of PGE₂ appears to be detrimental to the cell regenerative response, suggesting that NSAIDs are a possible therapeutic modality for restoring salivary gland function post-IR (Goldberg, 1986; Dennis and Norris, 2015; Gilman and Limesand, 2020).

While suppressing PGE₂ production appears to be protective for irradiated salivary glands (Figures 1, 2) (Gilman et al., 2019), how PGE₂ influences salivary gland dysfunction has not been clearly delineated. Previous work on pancreatitis, an inflammatory disorder that is associated with high serum amylase content, found that PGE₂ treatment blocks amylase secretion from pancreatic acini (Mössner et al., 1991). Furthermore, canines with allograft pancreatic transplants that were treated with dimethyl-PGE₂ had reduced amylase levels in urine compared to untreated controls, indicative of improved pancreatic function with PGE₂ (Garvin et al., 1989). Indomethacin treatment has been shown to increase isoproterenol (ISO)-induced amylase secretion from rat parotid gland tissue, where enhanced amylase secretion observed following ISO (0.1 μM) stimulation was abrogated by co-treatment with PGE₂ (Hata et al., 1990). Here, we show that PGE₂ treatment of primary parotid gland cells reduces amylase levels (Figures 5A,B) and that post-IR indomethacin treatment of mice increased amylase levels in whole parotid tissue (Figure 7). We also show that although carbachol-induced Ca²⁺ release from intracellular stores was unaffected, PGE₂ decreases SOCE in primary parotid gland cells (Figures 5C,D). Research on the mechanism whereby PGE₂ inhibits SOCE is limited, although studies have linked production of PGE₂ to activation of SOCE (Kuda et al., 2011; Jairaman et al., 2015). One previous study found that PGE₂ treatment (2 h) modulated

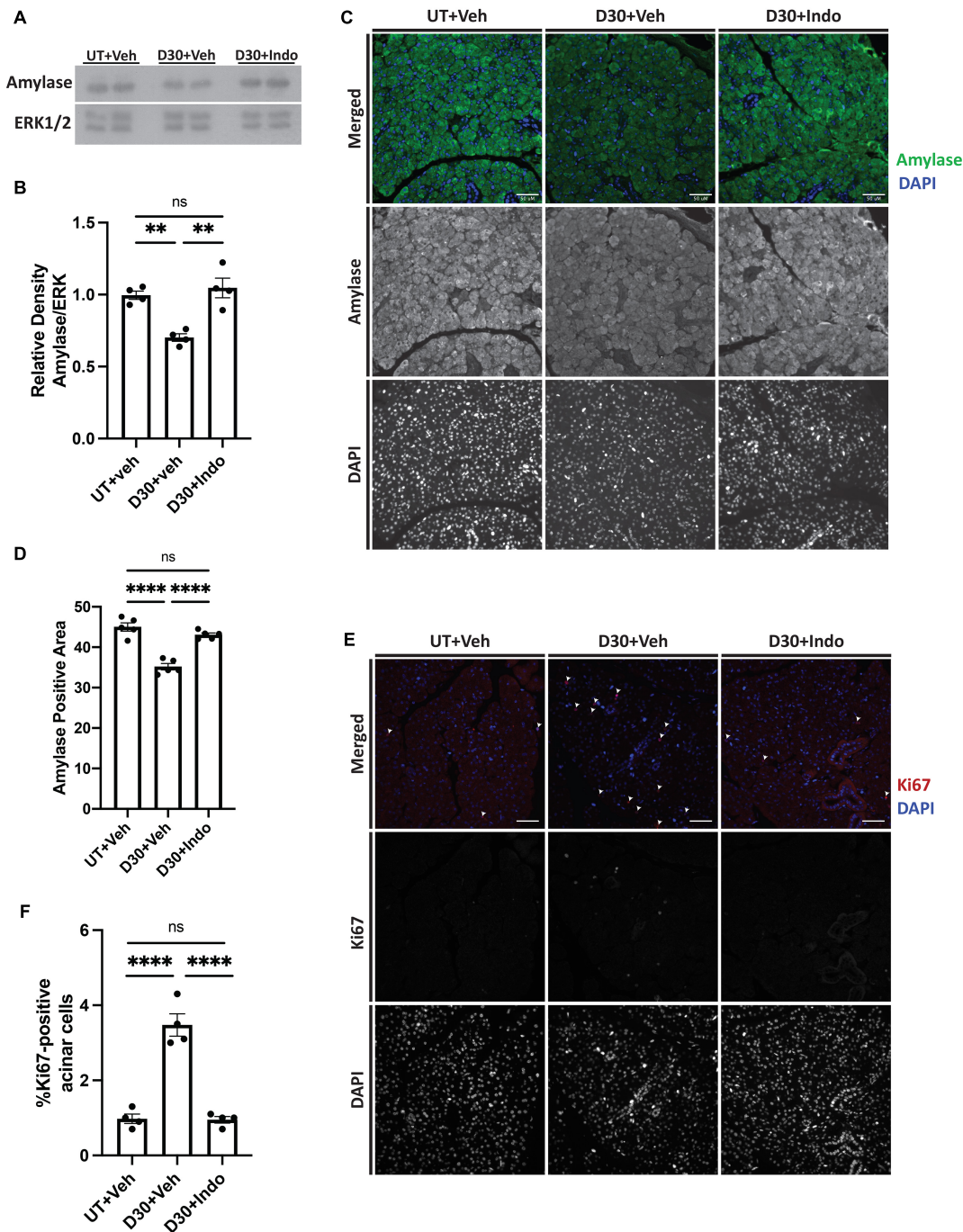


FIGURE 7 | Indomethacin treatment enhances amylase levels and reduces compensatory proliferation in whole parotid glands at day 30 post-IR. **(A,B)** C57BL/6J or **(C-F)** FVB mice were untreated (UT) or received 5 Gy ionizing radiation (IR) with intraperitoneal injections of vehicle (Veh, saline with 10% ethanol) or indomethacin (Indo, 1 mg/kg body weight) at days 3, 5, and 7 post-IR. Parotid glands were extracted at day 30 post-IR. **(A,B)** Immunoblots were generated from tissue lysates and an anti-amylase antibody, which were stripped and re-probed for ERK1/2 as a loading control. **(A)** Representative Western blot images of changes in amylase levels following radiation and indomethacin treatments. **(B)** Densitometry was performed using ImageJ software and protein content was normalized to the average of the UT + Veh group. **(C-F)** Parotid glands were fixed, sectioned and immunohistochemistry was performed with **(C,D)** an anti-amylase antibody or **(E,F)** an anti-Ki67 antibody, as described in section “Materials and Methods.” **(C)** Representative images of amylase positive area (40× magnification, scale bar: 50 μm). **(D)** Percent positive amylase area was determined using ImageJ software. The graph represents the amylase positive area as a percentage of the total area. **(E)** Representative images of Ki67 positive area (white arrows indicate Ki67+, DAPI+ cells; 40× magnification, scale bar: 50 μm). **(F)** Ki67 positive and total cell numbers were manually counted from 5 fields of view/mouse. The graph represents the Ki67 positive cell number as a percentage of the total cell number. **(B,D,F)** Graphs represent the mean ± SEM. Each closed circle represents an independent sample. Significant differences were determined via a one-way ANOVA followed by Bonferroni’s *post hoc* comparisons (***p* < 0.01, *****p* < 0.0001; ns = not significant).

T cell receptor activation-induced calcium mobilization and SOCE in T cells (Choudhry et al., 1999), which express all EPR isoforms (EP1-4Rs) (Nataraj et al., 2001). In the current study, we show that PGE₂ treatment (24 h) of primary mouse parotid cells that express EP1, EP2, EP3, and EP4 receptors (**Supplementary Figure 3**) had no effect on carbachol-induced release of intracellular stores but did reduce subsequent SOCE (**Figures 5C,D**). Radiation has been shown to cause a loss of SOCE in salivary gland cells due to STIM1 cleavage through activation of the TRPM2 pathway (Liu et al., 2017), although there have been no reports on interactions between PGE₂ and its receptors (EP1-EP4) and this pathway. Further investigation of how PGE₂ modulates amylase production and SOCE in salivary glands is warranted and this information may be applicable to other exocrine organs, such as the pancreas and lacrimal glands.

PGE₂ has been shown to activate the JNK/c-Jun pathway (Zeng et al., 2015; Arasa et al., 2019) and induces proliferation of pulmonary tumors (Zhong et al., 2015) and human mesenchymal stem cells (Yun et al., 2011). Previous work from our lab indicated that JNK/c-Jun activation leads to compensatory proliferation at day 5 post-IR (Wong et al., 2019) that remains elevated through day 90 (Grundmann et al., 2010) and reducing this dysregulated compensatory proliferation correlates with improved salivary gland function post-IR (Grundmann et al., 2010; Hill et al., 2014; Wong et al., 2019). The mediators responsible for radiation-induced cell proliferation in salivary glands are not well defined. Here, we show that PGE₂ treatment of primary parotid gland cells activates the JNK/c-Jun pathway (**Figure 3**) and PGE₂ or selective EP2, EP3, or EP4 receptor agonists induce cell proliferation (**Figure 4**), suggesting that PGE₂ mediates the compensatory proliferation response observed in parotid glands *in vivo*. Further supporting this observation, post-radiation indomethacin treatment significantly reduced JNK pathway activation in parotid glands of mice (**Figure 6**) and Ki67 positive staining at day 30 (**Figures 7E,F**), which correlates with the ability of indomethacin to improve salivary gland function in irradiated salivary glands (**Figures 1C–F**). Taken together, our data suggest that indomethacin treatment is a viable pharmacotherapeutic approach to protect salivary glands from IR-induced damage by blocking PGE₂ production and its activation of the JNK/c-Jun pathway leading to dysregulated proliferation. Relevantly, excessive PGE₂ production has been implicated in the progression of cancer (Nakanishi and Rosenberg, 2013). In multiple HNC models there is evidence that increased production of PGE₂ increases tumor cell proliferation that can be inhibited with NSAID treatment (Zweifel et al., 2002; Pelzmann et al., 2004; Ye et al., 2004). In HNC xenografts with head and neck squamous cell carcinoma-1483 (SCC-1483) cells, increased COX-2-mediated PGE₂ production was observed and treatment with a COX-2 selective inhibitor or a PGE₂-neutralizing antibody reduced tumor growth (Zweifel et al., 2002). Interestingly, treatment of oral SCC-25 cells with genistein, celecoxib or indomethacin reduced PGE₂ production and cell proliferation levels compared to controls (Ye et al., 2004). Lastly, indomethacin treatment of SCC-25 or SCC-9 cell lines reduced cell growth and induced apoptosis *in vitro* (Pelzmann et al., 2004). Therefore, the use of NSAIDs, such as

indomethacin, may be a general means to restrict the growth of cells that become dedifferentiated, as is the case with irradiated salivary gland acinar cells and metastatic tumor cells, both of epithelial origin.

DATA AVAILABILITY STATEMENT

The original contributions presented in the study are included in the article/**Supplementary Material**, and further inquiries can be directed to the corresponding author/s.

ETHICS STATEMENT

The animal study was reviewed and approved by the University of Arizona Institutional Animal Care and Use Committee.

AUTHOR CONTRIBUTIONS

KG curated and visualized data and drafted the manuscript. KG and JC designed and conducted the experiments. KG, KL, and GW obtained funding for completion of this work. All authors conceptualized experiments, edited the manuscript and approved the final version of the manuscript.

FUNDING

This work was supported by the NIH R01 grant DE023342 to KL and GW, and the F31 grant DE028737 to KG. The funding agency had no role in study design, data collection, data analysis, the decision to publish this study or the preparation of this manuscript.

ACKNOWLEDGMENTS

We would like to thank Sean Limesand for the use of the Leica DM5500 microscope and Partha Samadder for technical assistance.

SUPPLEMENTARY MATERIAL

The Supplementary Material for this article can be found online at: <https://www.frontiersin.org/articles/10.3389/fbioe.2021.697671/full#supplementary-material>

Supplementary Figure 1 | Additional doses of PGE₂ and EP2R, EP3R and EP4R agonists induce proliferation of primary parotid gland cells. Primary parotid cells were prepared from C57BL/6J mice, serum-starved for 2 h and treated with vehicle (DMSO), PGE₂ (0.03 μM), or EP-receptor-selective (EP2R-EP4R) agonists for EP2R: AH13205 (10 μM), EP3R: sulprostone (0.01 μM) or EP4R: CAY10598 (10 μM). All compounds were solubilized in DMSO, mixed with serum-free primary cell culture media and incubated with cells for 24 h with EdU added during the last hour of treatment to monitor proliferating cells, as described in section “Materials and Methods.” **(A)** Groups were quantified by averaging the number of positive cells out of the total number of cells from 5 fields of view/slide. Graphs represent the mean ± SEM. Each symbol represents an independent sample. Significant differences from DMSO-treated cells were determined via a one-way ANOVA

followed by Dunnett's *post hoc* comparisons (* $p < 0.05$, ** $p < 0.01$). **(B)** Representative fields of view are shown.

Supplementary Figure 2 | The effect of indomethacin treatment on AQP5 and MIST1 levels in irradiated parotid glands. **(A–C)** C57BL/6J mice were untreated (UT) or received 5 Gy ionizing radiation (IR) with intraperitoneal injections of vehicle (Veh, saline with 10% ethanol) or indomethacin (Indo, 1 mg/kg body weight) at days 3, 5, and 7 following IR and parotid glands were extracted at day 30. Immunoblots were generated from tissue lysates using anti-AQP5 or anti-MIST1 antibodies, and blots were stripped and re-probed for β -tubulin as a loading

control. **(A)** Representative Western blot of changes in AQP5 and MIST1 levels following radiation and indomethacin treatments. **(B,C)** Densitometry was performed using ImageJ software and protein content was normalized to the average of the UT + Veh group (* $p < 0.05$; ns = not significant).

Supplementary Figure 3 | EP1-4 receptors are present in murine parotid glands. Parotid glands were harvested from untreated (UT) C57BL/6J mice and used for immunoblots. The figure contains representative images of immunoblots for EPRs using antibodies against EP1R, EP2R, EP3R, and EP4R, which were stripped and re-probed for ERK1/2 as a loading control.

REFERENCES

- Arasa, J., Terencio, M. C., Andrés, R. M., Marín-Castejón, A., Valcuende-Cavero, F., Payá, M., et al. (2019). Defective induction of COX-2 expression by Psoriatic fibroblasts promotes pro-inflammatory activation of macrophages. *Front. Immunol.* 10:536. doi: 10.3389/fimmu.2019.00536
- Brown, W. A., Skinner, S. A., Malcontenti-Wilson, C., Vogliagis, D., and Brien, P. E. (2001). Non-steroidal anti-inflammatory drugs with activity against either cyclooxygenase 1 or cyclooxygenase 2 inhibit colorectal cancer in a DMH rodent model by inducing apoptosis and inhibiting cell proliferation. *Gut* 48, 660–666. doi: 10.1136/gut.48.5.660
- Choudhry, M. A., Hockberger, P. E., and Sayeed, M. M. (1999). PGE2 suppresses mitogen-induced Ca²⁺ mobilization in T cells. *Am. J. Physiol.* 277, R1741–R1748. doi: 10.1152/ajpregu.1999.277.6.R1741
- Cramer, J. D., Burtress, B., Le, Q. T., and Ferris, R. L. (2019). The changing therapeutic landscape of head and neck cancer. *Nat. Rev. Clin. Oncol.* 16, 669–683. doi: 10.1038/s41571-019-0227-z
- Dennis, E. A., and Norris, P. C. (2015). Eicosanoid storm in infection and inflammation. *Nat. Rev. Immunol.* 15, 511–523. doi: 10.1038/nri3859
- Garvin, P. J., Niehoff, M., and Burton, F. (1989). The effect of dimethyl PGE2 on canine pancreatic autograf exocrine secretion. *J. Surg. Res.* 46, 502–506. doi: 10.1016/0022-4804(89)90168-6
- Gilman, K. E., Camden, J. M., Klein, R. R., Zhang, Q., Weisman, G. A., and Limesand, K. H. (2019). P2X7 receptor deletion suppresses γ -radiation-induced hyposalivation. *Am. J. Physiol. Regul. Integr. Comp. Physiol.* 316, R687–R696. doi: 10.1152/ajpregu.00192.2018
- Gilman, K. E., and Limesand, K. H. (2020). The complex role of prostaglandin E(2)-EP receptor signaling in wound healing. *Am. J. Physiol. Regul. Integr. Comp. Physiol.* 320, R287–R296. doi: 10.1152/ajpregu.00185.2020
- Goldberg, R. I. (1986). Protection of irradiated parotid by prostaglandin synthesis inhibitors. *J. Am. Dent. Assoc.* 112, 179–181.
- Grundmann, O., Fillingner, J. L., Victory, K. R., Burd, R., and Limesand, K. H. (2010). Restoration of radiation therapy-induced salivary gland dysfunction in mice by post therapy IGF-1 administration. *BMC Cancer* 10:417. doi: 10.1186/1471-2407-10-417
- Grundmann, O., Mitchell, G. C., and Limesand, K. H. (2009). Sensitivity of salivary glands to radiation: from animal models to therapies. *J. Dent. Res.* 88, 894–903. doi: 10.1177/0022034509343143
- Hata, F., Takeuchi, T., Asano, M., and Yagasaki, O. (1990). Effects of indomethacin and prostaglandin E2 on amylase secretion by rat parotid tissue. *Biochem. Pharmacol.* 40, 390–393. doi: 10.1016/0006-2952(90)90707-R
- Hill, G., Headon, D., Harris, Z. I., Huttner, K., and Limesand, K. H. (2014). Pharmacological activation of the EDA/EDAR signaling pathway restores salivary gland function following radiation-induced damage. *PLoS One* 9:e112840. doi: 10.1371/journal.pone.0112840
- Jairaman, A., Yamashita, M., Schleimer, R. P., and Prakriya, M. (2015). Store-operated Ca²⁺ release-activated Ca²⁺ channels regulate PAR2-activated Ca²⁺ signaling and cytokine production in airway epithelial cells. *J. Immunol.* 195, 2122–2133. doi: 10.4049/jimmunol.1500396
- Jasmer, K. J., Gilman, K. E., Muñoz Forti, K., Weisman, G. A., and Limesand, K. H. (2020). Radiation-induced salivary gland dysfunction: mechanisms, therapeutics and future directions. *J. Clin. Med.* 9:4095. doi: 10.3390/jcm9124095
- Jensen, S. B., Vissink, A., Limesand, K. H., and Reyland, M. E. (2019). Salivary gland hypofunction and xerostomia in head and neck radiation patients. *J. Natl. Cancer Inst. Monogr.* 2019:lgz016. doi: 10.1093/jncimonographs/lgz016
- Jiang, J., Qiu, J., Li, Q., and Shi, Z. (2017). Prostaglandin E2 signaling: alternative target for glioblastoma? *Trends Cancer* 3, 75–78. doi: 10.1016/j.trecan.2016.12.002
- Johnson, D. E., Burtress, B., Leemans, C. R., Lui, V. W. Y., Bauman, J. E., and Grandis, J. R. (2020). Head and neck squamous cell carcinoma. *Nat. Rev. Dis. Primers* 6:92. doi: 10.1038/s41572-020-00224-3
- Johnson, G. L., and Nakamura, K. (2007). The c-jun kinase/stress-activated pathway: regulation, function and role in human disease. *Biochim. Biophys. Acta* 1773, 1341–1348. doi: 10.1016/j.bbamcr.2006.12.009
- Kuda, O., Jenkins, C. M., Skinner, J. R., Moon, S. H., Su, X., Gross, R. W., et al. (2011). CD36 protein is involved in store-operated calcium flux, phospholipase A2 activation, and production of prostaglandin E2. *J. Biol. Chem.* 286, 17785–17795. doi: 10.1074/jbc.M111.232975
- Liu, X., Gong, B., de Souza, L. B., Ong, H. L., Subedi, K. P., Cheng, K. T., et al. (2017). Radiation inhibits salivary gland function by promoting STIM1 cleavage by caspase-3 and loss of SOCE through a TRPM2-dependent pathway. *Sci. Signal.* 10:eal4064. doi: 10.1126/scisignal.aal4064
- Lombaert, I. M. A., Patel, V. N., Jones, C. E., Villier, D. C., Canada, A. E., Moore, M. R., et al. (2020). CERE-120 prevents irradiation-induced hypofunction and restores immune homeostasis in porcine salivary glands. *Mol. Ther. Methods Clin. Dev.* 18, 839–855. doi: 10.1016/j.omtm.2020.07.016
- Lucas, S. (2016). The pharmacology of indomethacin. *Headache* 56, 436–446. doi: 10.1111/head.12769
- Marmary, Y., Adar, R., Gaska, S., Wygoda, A., Maly, A., Cohen, J., et al. (2016). Radiation-induced loss of salivary gland function is driven by cellular senescence and prevented by IL6 modulation. *Cancer Res.* 76, 1170–1180. doi: 10.1158/0008-5472.CAN-15-1671
- Morgan-Bathke, M., Harris, Z. I., Arnett, D. G., Klein, R. R., Burd, R., Ann, D. K., et al. (2014). The Rapalogue, CCI-779, improves salivary gland function following radiation. *PLoS One* 9:e113183. doi: 10.1371/journal.pone.0113183
- Mössner, J., Secknus, R., Spiekermann, G. M., Sommer, C., Biernat, M., Bahnsen, H., et al. (1991). Prostaglandin E2 inhibits secretagogue-induced enzyme secretion from rat pancreatic acini. *Am. J. Physiol.* 260(Pt 1), G711–G719. doi: 10.1152/ajpgi.1991.260.5.G711
- Nakanishi, M., and Rosenberg, D. W. (2013). Multifaceted roles of PGE2 in inflammation and cancer. *Semin. Immunopathol.* 35, 123–137. doi: 10.1007/s00281-012-0342-8
- Nataraj, C., Thomas, D. W., Tilley, S. L., Nguyen, M. T., Mannon, R., Koller, B. H., et al. (2001). Receptors for prostaglandin E(2) that regulate cellular immune responses in the mouse. *J. Clin. Invest.* 108, 1229–1235. doi: 10.1172/JCI13640
- Pelzmann, M., Thurnher, D., Gedlicka, C., Martinek, H., and Knerer, B. (2004). Nimesulide and indomethacin induce apoptosis in head and neck cancer cells. *J. Oral Pathol. Med.* 33, 607–613. doi: 10.1111/j.1600-0714.2004.00216.x
- Reinke, J. M., and Sorg, H. (2012). Wound repair and regeneration. *Eur. Surg. Res.* 49, 35–43. doi: 10.1159/000339613
- Tanaka, A., Hase, S., Miyazawa, T., Ohno, R., and Takeuchi, K. (2002). Role of cyclooxygenase (COX)-1 and COX-2 inhibition in nonsteroidal anti-inflammatory drug-induced intestinal damage in rats: relation to various pathogenic events. *J. Pharmacol. Exp. Ther.* 303:1248. doi: 10.1124/jpet.102.041715
- Warner, T. D., Giuliano, F., Vojnovic, I., Bukasa, A., Mitchell, J. A., and Vane, J. R. (1999). Nonsteroid drug selectivities for cyclo-oxygenase-1 rather than cyclo-oxygenase-2 are associated with human gastrointestinal toxicity: a full in vitro analysis. *Proc. Natl. Acad. Sci. U. S. A.* 96, 7563–7568. doi: 10.1073/pnas.96.13.7563

- Wong, W. Y., Allie, S., and Limesand, K. H. (2019). PKC ζ and JNK signaling regulate radiation-induced compensatory proliferation in parotid salivary glands. *PLoS One* 14:e0219572. doi: 10.1371/journal.pone.0219572
- Woods, L. T., Camden, J. M., Khalafalla, M. G., Petris, M. J., Erb, L., Ambrus, J. L. Jr., et al. (2018). P2Y(2) R deletion ameliorates sialadenitis in IL-14 α -transgenic mice. *Oral Dis.* 24, 761–771. doi: 10.1111/odi.12823
- Ye, F., Wu, J., Dunn, T., Yi, J., Tong, X., and Zhang, D. (2004). Inhibition of cyclooxygenase-2 activity in head and neck cancer cells by genistein. *Cancer Lett.* 211, 39–46. doi: 10.1016/j.canlet.2004.03.043
- Yun, S. P., Ryu, J. M., Jang, M. W., and Han, H. J. (2011). Interaction of profilin-1 and F-actin via a β -arrestin-1/JNK signaling pathway involved in prostaglandin E(2)-induced human mesenchymal stem cells migration and proliferation. *J. Cell. Physiol.* 226, 559–571. doi: 10.1002/jcp.22366
- Zeng, C., Xu, J. N., Zhou, Y., Yang, H. X., Zhou, Y. F., and Xue, Q. (2015). C-Jun NH2-terminal kinase and p38 inhibition suppresses prostaglandin E2-stimulated aromatase and estrogen receptor levels in human endometriosis. *J. Clin. Endocrinol. Metab.* 100, E1404–E1414. doi: 10.1210/jc.2015-2031
- Zhao, Q., Zhang, L., Hai, B., Wang, J., Baetge, C. L., Deveau, M. A., et al. (2020). Transient activation of the Hedgehog-Gli pathway rescues radiotherapy-induced dry mouth via recovering salivary gland resident macrophages. *Cancer Res.* 80, 5531–5542. doi: 10.1158/0008-5472.CAN-20-0503
- Zhong, X., Fan, Y., Ritzenthaler, J. D., Zhang, W., Wang, K., Zhou, Q., et al. (2015). Novel link between prostaglandin E2 (PGE2) and cholinergic signaling in lung cancer: the role of c-Jun in PGE2-induced α 7 nicotinic acetylcholine receptor expression and tumor cell proliferation. *Thorac. Cancer* 6, 488–500. doi: 10.1111/1759-7714.12219
- Zweifel, B. S., Davis, T. W., Ornberg, R. L., and Masferrer, J. L. (2002). Direct evidence for a role of cyclooxygenase 2-derived prostaglandin E2 in human head and neck xenograft tumors. *Cancer Res.* 62, 6706–6711.

Conflict of Interest: The authors declare that the research was conducted in the absence of any commercial or financial relationships that could be construed as a potential conflict of interest.

Copyright © 2021 Gilman, Camden, Woods, Weisman and Limesand. This is an open-access article distributed under the terms of the Creative Commons Attribution License (CC BY). The use, distribution or reproduction in other forums is permitted, provided the original author(s) and the copyright owner(s) are credited and that the original publication in this journal is cited, in accordance with accepted academic practice. No use, distribution or reproduction is permitted which does not comply with these terms.